Spectrum of the Cavity-QED Microlaser: Strong Coupling Effects in the Frequency Pulling at Off Resonance

H.-G. Hong,[1] W. Seo,[1] Y. Song,[1] M. Lee,[1] H. Jeong,[1] Y. Shin,[1] W. Choi,[2] R. R. Dasari,[3] and K. An[1,*]

[1]*Department of Physics and Astronomy, Seoul National University, Seoul 151-747, Korea*

[2]*Department of Physics, Korea University, Seoul 136-701, Korea*

[3]*G. R. Harrison Spectroscopy Laboratory, Massachusetts Institute of Technology, Cambridge, Massachusetts 02139, USA*

(Received 4 June 2012; published 12 December 2012)

We report the first experimental observation of the cavity-QED microlaser spectrum, specifically the unconventional frequency pulling brought by a strong atom-cavity coupling at off resonance. The pulling is enhanced quadratically by the atom-cavity coupling to result in a sensitive response to the number of pumping atoms (2.1 kHz per atom maximally). Periodic variation of the pulling due to the coherent Rabi oscillation is also observed as the number of pumping atoms is increased across multiple thresholds.

DOI: 10.1103/PhysRevLett.109.243601 PACS numbers: 42.50.Pq, 42.50.Ar, 42.50.Gy, 42.50.Nn

Enhanced emission of photons under the strong coupling condition of the cavity quantum electrodynamics (QED) is the main mechanism behind the laser oscillations with a small number of emitters [1–5]. This class of lasers, the cavity-QED lasers, exhibit fundamental differences from the conventional laser in the threshold behavior and the intensity correlation function, in which a well-defined emitter-cavity coupling strength plays a significant role [6]. They are nonclassical light sources [7–9], not only providing a test ground of quantum optics [10] but finding applications as well in precision measurement [11] and low-noise communication [12]. Most previous investigations have been, however, limited to resonant interactions. The enhanced dispersive interaction at off resonance, widely studied in passive systems in the context of quantum information processing [13–16], has not been explored in the active radiation sources of cavity-QED yet.

The manifestation of the dispersive interaction in a laser is not apparent in the usual intensity-based measurements: the dispersive interaction induces a shift in the spectral contents of the radiation—namely the frequency pulling—owing to the continuous generation of phase shift by the pumping process [17]. In the cavity-QED lasers, the frequency pulling can be greatly enhanced in a nonlinear fashion by a strong emitter-cavity coupling g in contrast to the conventional laser showing no g dependence at all due to stochastic averaging [18]. Moreover, the spectrum is expected to show novel features due to the coherent Rabi oscillation as the pumping is increased [18–20], which cannot be explained by the standard theory of Schawlow and Townes.

Here, we report the first experimental observation of the cavity-QED microlaser spectrum at off resonance. Specifically, we observed the coupling-enhanced frequency pulling and its periodic variation with the increased pumping. For this, we performed the power spectral density measurement, a long-anticipated experimental task in the micromaser and microlaser physics [19]. While the micromaser requires the spectroscopy based on atomic state detection [19,21], whose experimental implementation is still elusive, the microlaser allows the use of a highly sensitive optical heterodyne technique called photon-counting-based second-order correlation spectroscopy (PCSOCS) [22,23]. In our experiment, we observed the frequency pulling enhanced nonlinearly as the atom-cavity coupling constant increased. The maximum amount of frequency pulling was a few kHz per atom, whereas it would be vanishingly small in the conventional laser. As a result, the differential pulling due to the intracavity atom-number distribution becomes the main source of the microlaser linewidth. In addition, periodic drop of the frequency pulling accompanied by abrupt increase of the intensity was observed at multiple thresholds [24] as the number of pumping atoms increased. This variation, arising from the coherent Rabi oscillation, contrasts to the constant frequency pulling in the conventional laser irrespective of the pumping [17].

The microlaser setup shown in Fig. 1(a) is basically identical to that employed in the previous works [9,24] except for the detection scheme designed for PCSOCS. The gain medium is provided by a collimated atomic beam of ^{138}Ba. The lasing occurs at the $\Delta m = 0$ transition of $^1S_0 - {}^3P_1$ (wavelength 791.1 nm), in which the spontaneous emission into noncavity free-space modes occurs at a rate of $\gamma_a/2\pi \simeq 25$ kHz (half linewidth). Just before entering the cavity mode, each atom is excited to the $^3P_1$ state by a pump laser polarized along the atomic beam direction. A magnetic field inducing a Zeeman shift of 80 MHz is applied in the same direction in order to define a quantization axis and to decouple the $m \neq 0$ sublevels from the cavity field. The Fabry-Perot cavity supports a transverse electromagnetic (TEM) Gaussian mode TEM_{00} with a waist 41 μm and a half linewidth $\gamma_c/2\pi = 91$ kHz. The average atom-cavity interaction time t_{int} is about 0.1 μs [25], which is much shorter than the decay time of the cavity as well as that of the excited atom.

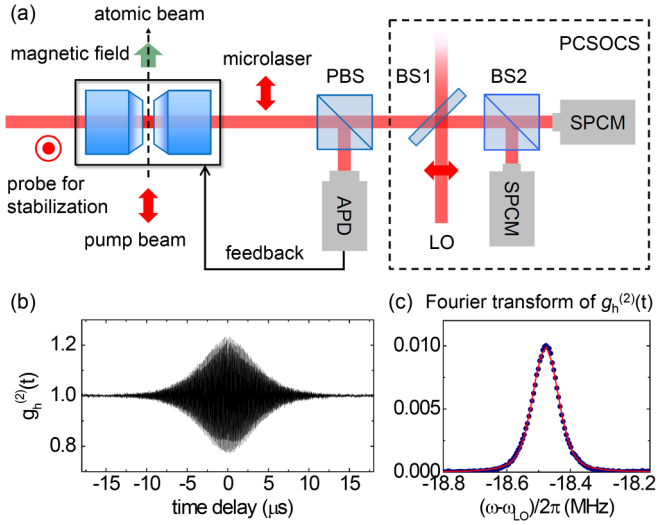

FIG. 1 (color online). (a) Schematic of the experimental setup. The polarizations, denoted by red arrows, of the microlaser and the cavity stabilization laser are orthogonal to each other. PBS: polarizing beam splitter, BS1: high transmission beam splitter, BS2: nonpolarizing beam splitter, APD: avalanche photodiode, SPCM: single photon counting module, LO: local oscillator. (b) The typical second-order correlation function $g_h^{(2)}(t)$ of the heterodyne signal. (c) The spectrum obtained by Fourier-transforming $g_h^{(2)}(t)$ in (b). The red solid curve is a fit with a Voigt integral function [18].

The atomic beam is intentionally tilted by about $\theta \simeq 20$ mrad with respect to the normal incidence in order to achieve spatially uniform atom-cavity interaction by decomposing the standing wave cavity mode into two Doppler-shifted traveling waves [26]. The corresponding Doppler shift $k\bar{v}\theta/2\pi$ is about ± 20 MHz (k: wave number, $\bar{v}$: mean velocity), producing two decoupled effective resonances [27]. Since those resonances form mirror images to each other, we explored only the down-shifted resonance throughout this work. The resonance frequency ω_0, to which the cavity-atom detuning Δ is defined hereafter, should be understood as the Doppler down-shifted one unless specified otherwise. The effective atom-cavity coupling rate $g_0/2\pi$ for each traveling wave resonance is 190 kHz, bigger than any dissipation rates, and thus, the system satisfies the strong coupling condition.

For PCSOCS, we construct the second-order correlation function of a heterodyne signal [22] obtained by overlapping a stable local oscillator (LO) laser with the microlaser radiation. A laser stabilized to the atomic resonance frequency (not Doppler shifted) by the frequency modulation spectroscopy [28] is used for the LO as well as the pump laser. The mode-matched LO and the microlaser are guided into two photon-counting avalanche photodiodes (APDs), each of which is the start and stop channel for constructing a second-order correlation histogram [29]. The temporal and spectral resolution of the current PCSOCS setup is 12.5 ns and 4.9 kHz, respectively.

The typical second-order correlation function is shown in Fig. 1(b), from which the power spectrum is obtained by Fourier transformation [22] as in Fig. 1(c). The beat frequency is the frequency difference between the microlaser oscillation and the LO frequency ω_{LO}, and the decay time corresponds to the inverse of the linewidth. The linewidth of the measured spectra contains a technical broadening (44 kHz) originating from a finite linewidth (22 kHz) of the LO laser and the cavity frequency jitter (38 kHz). Since the microlaser is operated around the Doppler shifted ($\simeq 20$ MHz) resonance with about ± 10 MHz detuning range as in Fig. 2(a), the resulting beating frequency varies from 10 MHz to 30 MHz depending on the detuning.

The cavity frequency ω_c is locked to an independently tunable probe laser which is also derived from the pump laser. Owing to the side-locking scheme, the frequencies of the probe and the cavity are offset by $\Delta_{pc}/2\pi \simeq 250$ kHz. The polarization of the probe is perpendicular to the quantization axis, minimizing its coupling to the microlaser transition [30]. The absorption of the probe by the atom is further minimized by the large Zeeman shift.

With the cavity locked with a detuning Δ, the microlaser output is spectrally analyzed by PCSOCS as shown in the example of Fig. 2(b). If the frequency pulling were absent, the spectral peak of the microlaser should appear at the passive cavity frequency indicated by the red dashed line. However, the measured spectral density is found to be pulled toward the atomic line center. The magnitude of the shift depends on the detuning, and if we plot the frequency pulling δ, defined as the center frequency of the spectrum minus ω_c, as a function of the detuning, we obtain a dispersion curve crossing zero at the atomic resonance frequency ω_0 [Fig. 2(c)]. The slight asymmetry with respect to the sign of the detuning results from the small remnants of the coupling between Doppler shifted traveling waves [27].

In the conventional laser theory, the notion of the emitter-cavity coupling constant does not appear in the frequency pulling which is solely determined by the bandwidths of the passive cavity and gain medium [17]. On the other hand, the frequency pulling in the cavity-QED microlaser [18] is given by

$$\delta \approx -\frac{\gamma_c \Delta}{t_{\mathrm{int}}^{-1}} \frac{\bar{N}}{\bar{N}_{\mathrm{th}}} \xi(\Phi), \tag{1}$$

where $\bar{N}_{\mathrm{th}} \equiv 2\gamma_c/g^2 t_{\mathrm{int}}$ denoting the threshold atom number in the cavity and $\xi(\Phi) \equiv (1 - \sin\Phi/\Phi)/\Phi^2$ with Φ being the precession angle of the Bloch vector including the detuning effect. The first factor $\gamma_c \Delta/t_{\mathrm{int}}^{-1}$ is nothing but the well-known frequency pulling of the conventional laser. The second factor $\bar{N}/\bar{N}_{\mathrm{th}}$ proportional to $\bar{N}g^2$ is an enhancement factor due to the strong atom-cavity coupling. The last factor $\xi(\Phi)$, a periodic function of Φ, comes from the precession of the Bloch vector. In the present

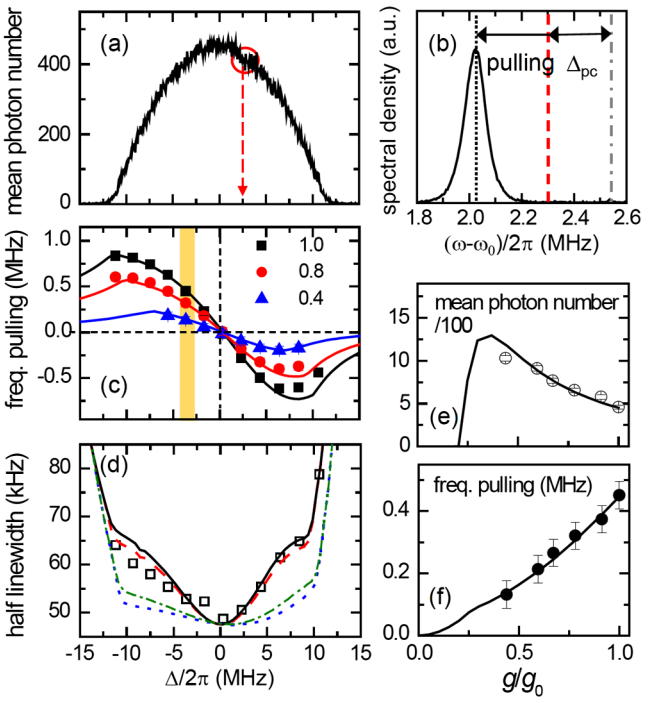

FIG. 2 (color online). (a) The mean photon number in the cavity obtained by scanning the cavity resonance frequency. Indicated by the red circle is the fixed cavity frequency for the example of (b). (b) At the fixed cavity frequency the spectral contents of the microlaser emission is obtained by PCSOCS. The red dashed line indicates the cold cavity frequency which is offset from the probe frequency (gray dashed-dotted line). The black dotted line is the center frequency of the microlaser. (c) The frequency pulling extracted from the analysis like (b) as a function of the cavity-atom detuning for the selected values of g/g_0 indicated in the panel. The symbols correspond to the experiment, and the curves to the theory. (d) The linewidth obtained by fitting the spectra for $g = g_0$ (empty square). The theoretical curves are obtained by considering the nondispersive effect only (blue dotted line), including the differential pulling induced by Δn (green dashed-dotted line), including the differential pulling induced by ΔN (red dashed line) and including the effect of both ΔN and Δn (black solid line). (e) The mean photon number on resonance as we increase the effective coupling constant. (f) The amount of the frequency pulling as a function of g/g_0 at the detuning (-3.6 MHz) denoted with a yellow bar in (c). The filled circles are from the experiment. The solid curves in (e) and (f) are from the quantum theory. The velocity of the atom follows a Gaussian distribution with $\bar{v} = 680$ m/s and $\Delta v_{\mathrm{FWHM}}/\bar{v} \simeq 0.35$. The associated Doppler shift is 20.5 MHz.

experiment, $\bar{N}/\bar{N}_{\mathrm{th}}$ can exceed 20 with $\xi(\Phi)$ being of order of 0.1.

In our experiment, we can systematically control the degree of atom-cavity coupling and investigate its effect on the frequency pulling. Owing to the Gaussian transverse profile of the cavity mode, we can change the ratio of g to the maximum achievable coupling g_0 by adjusting the vertical position of the incoming atoms with an atom-beam aperture of a rectangular opening with a vertical full width of 25 μm. The intracavity mean atom number $\bar{N}$ is made large enough ($\bar{N} = 250$) so that the microlaser with g_0 operates well above the threshold on resonance. As we move the position of the atomic beam away from the mode center, the gradual increase of the mean photon number in the cavity is observed until the effective coupling goes below a critical value of about $0.25g_0$, below which the lasing stops as depicted in Fig. 2(e).

We recorded the spectrum for various detunings to obtain the frequency pulling curves as in Fig. 2(c). In contrast to the mean photon number, the amount of the frequency pulling diminishes with the reduction of g/g_0. The quantum theory of Ref. [18] predicts the presence of an inflection point at the critical value of g and the scaling of the pulling to be approximately $(g/g_0)^2$, consistent with Eq. (1), branching from the critical point. At a fixed detuning indicated by a yellow bar in Fig. 2(c), the detailed variation of the pulling is shown in Fig. 2(f). The data are not available below the critical point since they require a data acquisition time too long for a finite oven lifetime. Above the critical point the observed frequency pulling clearly demonstrates the effect of $\bar{N}/\bar{N}_{\mathrm{th}}$ in Eq. (1).

The frequency pulling also plays a significant role in the microlaser linewidth. The sensitive dependence of the spectral shift on the number of pumping atoms, to be seen below in Fig. 3(a), gives rise to a spectral broadening associated with the intrinsic Poissonian atom-number distribution P_N for a given intracavity mean atom number $\bar{N}$. It has also been speculated that a broadening can emerge from the photon-number-dependent frequency pulling associated with the photon number distribution P_n at a fixed atom number N [18]. In the current experimental setting, however, the atom number distribution turns out to be a major source of the spectral broadening due to the N dependence of the frequency pulling. We compare the experimental linewidth with the calculated line broadening associated with P_n with its spread Δn and P_N with ΔN in Fig. 2(d). The inclusion of ΔN in the theory much improves the agreement with the data, reproducing its typical V-shaped detuning curve. We cannot, however, resolve the contribution of either photon-number distribution or nondispersive phase diffusion [19] unambiguously with the present experimental precision.

The frequency pulling was measured as a function of the pumping or the mean atom number $\bar{N}$ in the cavity for $g = g_0$ as shown in Fig. 3. When $\bar{N}$ is increased, the system is expected to go through multiple thresholds at which the mean photon number suddenly jumps from one stable level to another, called the multiple branch solutions [24]. In order to quantify the sensitive response of the pulling to a small number of atoms we first investigate the regime of the first branch solution. At the detuning of 4.4 MHz around which the maximum pulling is achieved, the increase of the pulling as a function of $\bar{N}$ is plotted in Fig. 3(a). Although the curve is mildly nonlinear near the

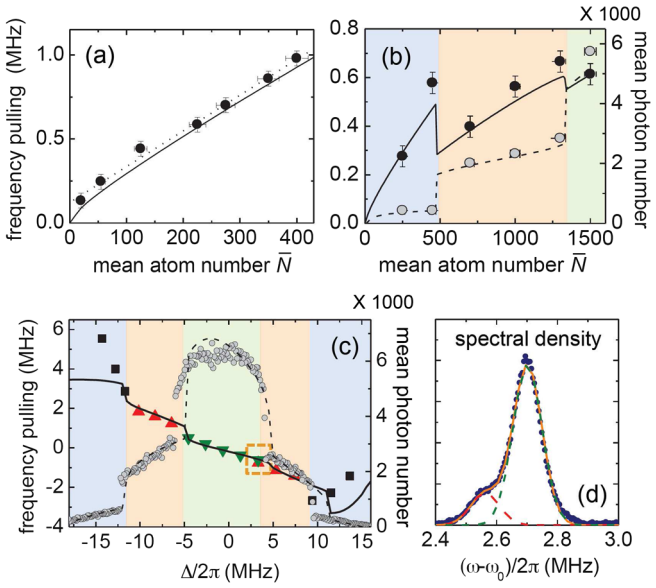

FIG. 3 (color online). (a) The magnitude of the frequency pulling at a fixed detuning of 4.6 MHz investigated within the first branch solution. The mean velocity $\bar{v}$ of atoms is 680 m/s with the inhomogeneous spread $\Delta v_{\mathrm{FWHM}}/v_c \simeq 0.35$ for this particular data. (circles: experiment, solid curve: theory, dotted line: linear fit) (b) The magnitude of the pulling (black circles: experiment, solid curve: theory) and the mean photon number (gray circles: experiment, dashed curve: theory) at a detuning of 3.3 MHz, here investigated up to the third branch solution. (c) The detuning curve of the mean photon number (gray circles) and the frequency pulling (squares: 1st, upright triangles: 2nd, inverted triangles: 3rd branch solution) with $\bar{N} = 1500$, at which the third branch solution is possible near resonance. (d) The spectrum taken at a detuning of 3.3 MHz [marked by the dashed box in (c)] is fitted by two Gaussian functions (dashed lines: individual Gaussian profiles, solid line: complete fitting). From (b) to (d) the atomic beam has $\bar{v} = 720$ m/s, $\Delta v_{\mathrm{FWHM}}/\bar{v} = 0.40$, and the associated Doppler shift is 21.5 MHz.

first threshold ($\bar{N} \sim 20$), a linear fit with a slope of $2.1(\pm 0.1)$ kHz per atom seems a good approximation. The system with the larger vacuum Rabi angle gt_{int} would further enhance the sensitivity of the frequency shift to a small number of atoms due to $\bar{N}/\bar{N}_{\mathrm{th}}$ factor in Eq. (1).

At the critical numbers of pumping atoms associated with the multiple thresholds, the microlaser is subject to a transition to the next branch solution via the tunneling of the photon number distribution [31,32]. Above the second threshold, the Bloch vector representing the quantum state of the gain medium precesses, in the course of the interaction, more than one cycle from its initially inverted state. The induced atomic polarization is thus brought back to zero and grows all over again. By this process the dispersive component of the induced polarization is reduced while the (negatively) absorptive component, which increases the emission probability, grows. Consequently, the amount of the pulling drops whereas the mean photon number shows a sudden rise at this transition. In Fig. 3(b) we present the aforementioned periodic variation, associated with the $\xi(\Phi)$ factor in Eq. (1), observed as a function of the pumping. This periodic variation, resulting from the unitary evolution of the atomic state in the strong coupling regime of the cavity-QED, is nonexistent in other dispersive systems relying on the Kerr effect or the ac Stark shift, for example. We also note that the amount of the frequency pulling in the Scully-Lamb conventional laser theory is clamped at a constant value of $-\frac{\gamma_c}{2\gamma_p}\Delta$, equivalent to the first factor in Eq. (1), where γ_p is the dephasing rate of the gain medium [17]. We would recover the result of the conventional laser when Eq. (1) and the microlaser result were averaged over a stochastic interaction time spoiling the well-defined atom-cavity coupling [17,18].

At a fixed large-enough $\bar{N}$, the system can stay in different branch solutions depending on the detuning Δ. For example, three possible branch solutions appear with Δ in Fig. 3(c). As we tune the cavity frequency, we then obtain multiple dispersion curves with the weaker dispersion at the higher branch solution. At the critical detuning, where both branch solutions are equally probable, the microlaser output exhibits a random-telegraphlike behavior with a period of hundreds of milliseconds, and consequently, the resulting spectrum is doubly peaked as shown in Fig. 3(d). This illustrates that the switching of the laser intensity by the quantum tunneling at off resonance in the microlaser accompanies the switching of its color.

In conclusion, we have observed the off resonance emission spectrum of the cavity-QED microlaser. The spectrum exhibited a spectral shift toward the atomic line center. The frequency pulling was quadratically enhanced by the strong and well-defined atom-cavity coupling, resulting in a detectable per-atom frequency shift and a consequent line broadening arising from the intrinsic intracavity atom number distribution. Negligible decoherence of the atomic state during the interaction time also led to the periodic rise and fall of the frequency puling associated with the Rabi oscillation as the pumping was increased. The frequency pulling is expected to cancel out the cavity-atom detuning when $\bar{N}(gt_{\mathrm{int}})^2 \ggg 1$ [18], and thus, the lasing frequency becomes insensitive to the cavity frequency fluctuation, which may help the stability of optical clocks [33].

This work was supported by the National Research Foundation (Grants No. WCU-R32-10045 and No. 20110015720).

*kwan@phya.snu.ac.kr

[1] D. Meschede, H. Walther, and G. Müller, Phys. Rev. Lett. **54**, 551 (1985).
[2] K. An, J. J. Childs, R. R. Dasari, and M. S. Feld, Phys. Rev. Lett. **73**, 3375 (1994).
[3] J. McKeever, A. Boca, A. D. Boozer, J. R. Buck, and H. J. Kimble, Nature (London) **425**, 268 (2003).

[4] O. Astafiev, K. Inomata, A. O. Niskanen, T. Yamamoto, Yu. A. Pashkin, Y. Nakamura, and J. S. Tsai, Nature (London) **449**, 588 (2007).
[5] M. Nomura, N. Kumagai, S. Iwamoto, Y. Ota, and Y. Arakawa, Nat. Phys. **6**, 279 (2010).
[6] F. Dubin, C. Russo, H. G. Barros, A. Stute, C. Becher, P. O. Schmidt, and R. Blatt, Nat. Phys. **6**, 350 (2010).
[7] G. Rempe, F. Schmidt-Kaler, and H. Walther, Phys. Rev. Lett. **64**, 2783 (1990).
[8] M. Weidinger, B. T. H. Varcoe, R. Heerlein, and H. Walther, Phys. Rev. Lett. **82**, 3795 (1999).
[9] W. Choi, J.-H. Lee, K. An, C. Fang-Yen, R. R. Dasari, M. S. Feld, Phys. Rev. Lett. **96**, 093603 (2006).
[10] G. Rempe, H. Walther, and N. Klein, Phys. Rev. Lett. **58**, 353 (1987).
[11] D. Meiser, J. Ye, D. R. Carlson, and M. J. Holland, Phys. Rev. Lett. **102**, 163601 (2009).
[12] L. Davidovich, Rev. Mod. Phys. **68**, 127 (1996).
[13] Q. A. Turchette, C. J. Hood, W. Lange, H. Mabuchi, and H. J. Kimble, Phys. Rev. Lett. **75**, 4710 (1995).
[14] A. Rauschenbeutel, G. Nogues, S. Osnaghi, P. Bertet, M. Brune, J. M. Raimond, and S. Haroche, Phys. Rev. Lett. **83**, 5166 (1999).
[15] D. I. Schuster, A. A. Houck, J. A. Schreier, A. Wallraff, J. M. Gambetta, A. Blais, L. Frunzio, J. Majer, B. Johnson, M. H. Devoret, S. M. Girvin, and R. J. Schoelkopf, Nature (London) **445**, 515 (2007).
[16] I. Fushman, D. Englund, A. Faraon, N. Stoltz, P. Petroff, and J. Vučković, Science **320**, 769 (2008).
[17] M. O. Scully and M. S. Zubairy, *Quantum Optics* (Cambridge University Press, Cambridge, England, 1997).
[18] H.-G. Hong and K. An, Phys. Rev. A **85**, 023836 (2012).
[19] M. O. Scully, H. Walther, G. S. Agarwal, T. Quang, and W. Schleich, Phys. Rev. A **44**, 5992 (1991).
[20] M. Loffler, G. M. Meyer, and H. Walther, Phys. Rev. A **55**, 3923 (1997).
[21] F. Casagrande, A. Ferraro, A. Lulli, R. Bonifacio, E. Solano, and H. Walther, Phys. Rev. Lett. **90**, 183601 (2003).
[22] H.-G. Hong, W. Seo, M. Lee, W. Choi, J.-H. Lee, and K. An, Opt. Lett. **31**, 3182 (2006).
[23] W. Kim, C. Park, J.-R. Kim, Y. Choi, S. Kang, S. Lim, Y.-L. Lee, J. Ihm, and K. An, Nano Lett. **11**, 729 (2011).
[24] C. Fang-Yen, C. C. Yu, S. Ha, W. Choi, K. An, R. R. Dasari, and M. S. Feld, Phys. Rev. A **73**, 041802(R) (2006).
[25] Because of the finite lifetime of the atomic oven, several ovens with slightly different t_{int}, which is specified for each data set, were employed to cover the parameter range in this work.
[26] K. An, R. R. Dasari, and M. S. Feld, Opt. Lett. **22**, 1500 (1997).
[27] H.-G. Hong, W. Seo, M. Lee, Y. Song, W. Choi, C. Fang-Yen, R. R. Dasari, M. S. Feld, J.-H. Lee, and K. An, Phys. Rev. A **79**, 033816 (2009).
[28] K. An, R. R. Dasari, and M. S. Feld, Appl. Phys. Lett. **66**, 2162 (1995).
[29] W. Choi, M. Lee, Y.-R. Lee, C. Park, J.-H. Lee, and K. An, Rev. Sci. Instrum. **76**, 083109 (2005).
[30] Unfortunately, the high-finesse cavity itself is a weak depolarizing element, and thus, about 2% of the probe power, corresponding to a mean photon number of about 2, is converted to the microlaser polarization, providing a coherent injection seeding when the probe and the microlaser have a spectral overlap. For most of the tuning range, however, such an overlap is avoided because of the narrow linewidth of the microlaser spectrum compared to the separation from the probe frequency, and thus the probe just leaves a small peak used as a frequency marker as in Fig. 2(b).
[31] P. Filipowicz, J. Javanainen, and P. Meystre, Phys. Rev. A **34**, 3077 (1986).
[32] O. Benson, G. Raithel, and H. Walther, Phys. Rev. Lett. **72**, 3506 (1994).
[33] J. G. Bohnet, Z. Chen, J. M. Weiner, D. Meiser, M. J. Holland, and J. K. Thompson, Nature (London) **484**, 78 (2012).